

Revisit local spin polarization beyond global equilibrium in relativistic heavy ion collisions

Cong Yi^{*} and Shi Pu[†]

*Department of Modern Physics, University of Science
and Technology of China, Hefei, Anhui 230026, China*

Di-Lun Yang[‡]

Institute of Physics, Academia Sinica, Taipei, 11529, Taiwan

Abstract

We have studied local spin polarization in the relativistic hydrodynamic model. Generalizing the Wigner functions previously obtained from chiral kinetic theory in Ref. [1] to the massive case, we present the possible contributions up to the order of \hbar from thermal vorticity, shear viscous tensor, other terms associated with the temperature and chemical-potential gradients, and electromagnetic fields to the local spin polarization. We then implement the (3+1) dimensional viscous hydrodynamic model to study the spin polarizations from these sources with a small chemical potential and ignorance of electromagnetic fields by adopting an equation of state different from those in other recent studies. Although the shear correction alone upon local polarization results in the sign and azimuthal-angle dependence more consistent with experimental observations, as also discovered in other recent studies, it is mostly suppressed by the contributions from thermal vorticity and other terms that yield an opposite trend. It is found that the total local spin polarization could be very sensitive to the equation of states, the ratio of shear viscosity over entropy density, and freezeout temperature.

^{*}Electronic address: congyi@mail.ustc.edu.cn

[†]Electronic address: shipu@ustc.edu.cn

[‡]Electronic address: dlyang@gate.sinica.edu.tw

I. INTRODUCTION

In non-central heavy-ion collisions, large orbital angular momenta (OAM) can be generated and transferred to the quark gluon plasma (QGP) in the form of vorticity fields. Proposed by Liang and Wang [2, 3] in early pioneer works, the global OAM could trigger the spin polarization of interacting partons through spin-orbit coupling. The magnitude of vorticity can be accordingly extracted through the spin polarization of hadrons created from the experiments. Later on, relativistic fermions with spin in thermal equilibrium have been systematically studied in the statistical model and a more precise relation to the possible experimental observation has been established [4–6]. On the other hand, the properties and dynamical evolution of vorticity are further analyzed via numerical simulations in AMPT and HIJING [7–9]. Assuming the global equilibrium condition and employing the modified Cooper-Frye formula for spin polarization [6, 10], the spin polarization of Λ hyperons in heavy ion collisions has been estimated based on UrQMD [11] and hydrodynamic models [12–16]. See also Refs. [17–20] for other related studies. The theoretic predictions and follow-up studies [9, 11, 21–24] remarkably agree with the later measurement of the global polarization for Λ and $\bar{\Lambda}$ hyperons by STAR collaboration [25]. It is also shown an average angular velocity or vorticity of QGP is as large as $\omega \sim 10^{22} s^{-1}$ [25], which reveals that the QGP could be the most vortical fluid so far.

Despite the agreement between theory and experiment in global polarization, STAR collaboration has also measured the azimuthal angle dependence of the spin polarization along the beam and the out-plane directions in Au+Au collisions at 200 GeV [26, 27], known as the longitudinal and transverse local spin polarization, respectively. Most of theoretical simulations, e.g. relativistic hydrodynamics [28, 29] and transport models [11, 22, 30] failed to describe the measurements of local polarization with a few exception such as the numerical simulation from the kinetic theory of massless fermions in Ref. [31] and results from some phenomenological models in Ref. [16, 32, 33]. In general, these theoretical estimations have found the local polarization with an opposite sign against the experimental result. Also, the feed-down effects are found to be negligible for recoiling the tension [34, 35]. This disagreement between theory and the experiment for local spin polarization is dubbed as the “sign” problem.

Since most of the previous simulations rely on the assumption that spin polarization for

Λ hyperons at the freezeout hypersurface is mainly induced by the thermal vorticity in light of the statistical model [6] and Wigner-function approach [36] in global equilibrium, it is generally believed that the non-equilibrium effects beyond the assumption for global equilibrium is essential to delineate the local spin polarization. Consequently, many theoretical efforts have been inputted to study dynamical spin polarization. One microscopic theory for tracking the dynamical evolution of spin transport for relativistic fermion is the quantum kinetic theory (QKT). The QKT was developed for the massless fermions [1, 37–52] at the very beginning, known as the chiral kinetic theory (CKT). To describe the spin dynamics in particular for strange (s) quarks or Λ hyperons, QKT has been extended to the case for massive fermions [53–65]. In Ref. [66], another microscopic model for spin polarization through particle collisions is proposed. As for the macroscopic descriptions, one may need to add the spin effects to the relativistic hydrodynamics, i.e. relativistic spin hydrodynamics [67–77]. It has been derived from many approaches, e.g. the entropy principle [72, 78, 79], the Lagrangian effective theory [75, 76], kinetic approaches [67, 68, 70, 71, 73, 74], and general discussion from field theory [80]. Also, see recent reviews [81–85] and the references therein.

Nevertheless, to simulate the spin polarization of relativistic fermions far from equilibrium is technically difficult and computationally expensive. It is instead natural to explore the spin polarization near local equilibrium. From the detailed balance of massless fermions with 2-to-2 scattering in CKT, it has been shown that the Wigner function pertinent to spin polarization contains several corrections besides the thermal vorticity in local equilibrium as derived by some of the authors of this paper [1] in 2017. Recently, the authors in Refs. [86, 87] have found similar contributions for massive fermions in local equilibrium, which have smooth connection to part of the massless result. Based on their findings with peculiarly the shear correction, the hydrodynamic simulations in Ref. [88] show qualitative agreement with experimental data by computing the polarization of s quarks in Λ hyperons. Simultaneously, the authors in Ref. [89] have added the contribution from shear viscous tensor to the local spin polarization near isothermal equilibrium, in which the numerical results also agree with the experimental data qualitatively.

A natural question then arises: whether the numerical finding above with the shear corrections is sensitive to the parameters chosen in the hydrodynamics simulations? If the answer is positive, it implies that the correct "sign" for local polarization may not be solely

attributed to the shear correction in local equilibrium and further non-equilibrium corrections depending on interaction should be considered. Therefore, we follow the early work [1] done by some of the authors in the present paper and list all possible local-equilibrium corrections to the local spin polarization up to the order of \hbar . We then implement $(3+1)$ -dimensional viscous hydrodynamics to investigate the polarization induced by these effects. In order to examine the dependence of the numerical parameters in simulations, we use a different equation of states (EoS) as opposed to the one adopted in Ref. [88] and discuss the dependence of freezeout temperature and the ratio of shear viscosity to entropy density.

The structure of the paper is as follows. In Sec. II, we review the main results in our early work [1] and present all possible corrections in local equilibrium to polarization up to the order of \hbar explicitly. After that, we implement the viscous hydrodynamical simulations with AMPT initial condition to study the polarization and discuss the dependence of freezeout temperature and the ratio of shear viscosity to entropy density in Sec. III. We summarize in Sec. IV.

Through out this paper, we use the Minkowski metric $g_{\mu\nu} = \text{diag}\{+, -, -, -\}$ and define the Levi-Civita tensor $\epsilon^{\mu\nu\alpha\beta}$ with the convention $\epsilon^{0123} = -\epsilon_{0123} = 1$. We also introduce the notations $A_{(\rho}B_{\sigma)} \equiv (A_\rho B_\sigma + A_\sigma B_\rho)/2$ and $A_{[\rho}B_{\sigma]} \equiv (A_\rho B_\sigma - A_\sigma B_\rho)/2$.

II. THEORETICAL ANALYSIS FROM QUANTUM KINETIC THEORIES

We are interested in the polarization (pseudo) vector characterized by the axial-charge current density in phase space,

$$\mathcal{J}_5^\mu(p, X) \equiv 2 \int_{p \cdot n} [\mathcal{J}_+^\mu(p, X) - \mathcal{J}_-^\mu(p, X)], \quad (1)$$

where $\int_{p \cdot n} \equiv \int dp \cdot n \theta(p \cdot n)/(2\pi)$ with $\theta(p \cdot n)$ an unit-step function¹. Here $\mathcal{J}_+^\mu(p, X)$ and $\mathcal{J}_-^\mu(p, X)$ denote the Wigner functions for right and left-handed fermions, respectively. Given $\mathcal{J}_5^\mu(p, X)$, we can calculate the spin polarization of Λ hyperons via the modified Cooper-Frye formula [6],

$$\mathcal{S}^\mu(\mathbf{p}) = \frac{\int d\Sigma \cdot p \mathcal{J}_5^\mu(p, X)}{2m_\Lambda \int d\Sigma \cdot \mathcal{N}(p, X)}, \quad (2)$$

¹ For the computation of spin polarization, we usually apply the on-shell Wigner functions. Here we thus integrate over the energy defined as $p \cdot n$, where n^μ may be chosen as the fluid four velocity in thermal equilibrium. Also, we further introduce a unit-step function to omit the contribution from anti-fermions.

where $\mathcal{N}^\mu(p, X) \equiv 2 \int_{p \cdot n} [\mathcal{J}_+^\mu(p, X) + \mathcal{J}_-^\mu(p, X)]$ is the number density in phase space and m_Λ is the mass of Λ and Σ_μ is the normal vector of the freezeout surface.

As derived in the early work [1], the Wigner functions for right or left-handed fermions near local equilibrium are given by ²

$$\mathcal{J}_\lambda^\mu(p, X) = 2\pi \text{sign}(u \cdot p) \left\{ p^\mu + \lambda \frac{\hbar}{2} \delta(p^2) [u^\mu(p \cdot \omega) - \omega^\mu(u \cdot p) - 2S_{(u)}^{\mu\nu} \tilde{E}_\nu] \partial_{u \cdot p} + \lambda \frac{\hbar}{4} \epsilon^{\mu\nu\alpha\beta} F_{\alpha\beta} \partial_\nu^p \delta(p^2) \right\} f_\lambda^{(0)}, \quad (3)$$

where $\lambda = \pm$ for right and left handed fermions, u^μ the fluid four velocity,

$$S_{(u)}^{\mu\nu} = \epsilon^{\mu\nu\alpha\beta} p_\alpha u_\beta / (2u \cdot p),$$

$$\tilde{E}_\nu = E_\nu + T \partial_\nu \frac{\mu_\lambda}{T} + \frac{(u \cdot p)}{T} \partial_\nu T - p^\sigma [\partial_{<\sigma} u_{\nu>} + \frac{1}{3} \Delta_{\sigma\nu} (\partial \cdot u) + u_\nu D u_\sigma]. \quad (4)$$

and

$$f_\lambda^{(0)} = 1 / (e^{(u \cdot p - \mu_\lambda)/T} + 1), \quad (5)$$

is the distribution function with T local temperature, and μ_\pm chemical potentials for right or left-handed fermions, respectively. In general, f_λ should incorporate non-equilibrium corrections depending on interaction to satisfy the kinetic equation near local equilibrium, while the corrections are expected to be higher orders in the gradient expansion and omitted here for simplicity [1, 90]. Here, electromagnetic fields are defined in the fluid-rest frame,

$$E_\mu \equiv u^\nu F_{\mu\nu}, \quad B^\mu \equiv \frac{1}{2} \epsilon^{\mu\nu\alpha\beta} u_\nu F_{\alpha\beta}. \quad (6)$$

We also decompose the derivative of u_ν as

$$\partial_\mu u_\nu = \partial_{<\mu} u_{\nu>} + u_\mu D u_\nu + \frac{1}{3} \Delta_{\mu\nu} (\partial \cdot u) + \omega_{\mu\nu}, \quad (7)$$

where

$$\Delta^{\mu\nu} = g^{\mu\nu} - u^\mu u^\nu, \quad (8)$$

is the projector,

$$D \equiv u \cdot \partial, \quad (9)$$

² In general, there exist off-equilibrium corrections pertinent to collisions, which are however higher-order in gradient expansion starting from $\mathcal{O}(\partial)$ and $\mathcal{O}(\partial^2)$ for parity even and odd terms, respectively. These corrections are neglected here.

$A^{<\mu\nu>}$ is the traceless part of an arbitrary tensor $A^{\mu\nu}$,

$$A^{<\mu\nu>} \equiv \frac{1}{2}[\Delta^{\mu\alpha}\Delta^{\nu\beta} + \Delta^{\nu\beta}\Delta^{\mu\alpha}]A_{\alpha\beta} - \frac{1}{3}\Delta^{\mu\nu}\Delta^{\alpha\beta}A_{\alpha\beta}, \quad (10)$$

and $\omega^{\mu\nu}$ is the vorticity tensor

$$\omega_{\alpha\beta} = \epsilon_{\alpha\beta\mu\nu}u^\mu\omega^\nu + \frac{1}{2}(u_\alpha Du_\beta - u_\beta Du_\alpha), \quad (11)$$

with vorticity defined as,

$$\omega^\mu = \frac{1}{2}\epsilon^{\mu\nu\alpha\beta}u_\nu\partial_\alpha u_\beta. \quad (12)$$

Using the following relation,

$$u^\mu(p \cdot \omega) - \omega^\mu(u \cdot p) = -\frac{1}{2}\epsilon^{\mu\nu\alpha\beta}p_\nu\partial_\alpha u_\beta + \frac{1}{2}\epsilon^{\mu\nu\alpha\beta}p_\nu u_\alpha Du_\beta, \quad (13)$$

we find

$$\begin{aligned} & u^\mu(p \cdot \omega) - \omega^\mu(u \cdot p) - 2S_{(u)}^{\mu\nu}\tilde{E}_\nu \\ &= -\frac{1}{2}\epsilon^{\mu\nu\alpha\beta}p_\nu T\partial_\alpha \frac{u_\beta}{T} + \frac{1}{2}\epsilon^{\mu\nu\alpha\beta}p_\nu u_\alpha Du_\beta - \frac{1}{2}\epsilon^{\mu\nu\alpha\beta}p_\alpha u_\beta \frac{1}{T}\partial_\nu T \\ & \quad - \frac{1}{(u \cdot p)}\epsilon^{\mu\nu\alpha\beta}p_\alpha u_\beta E_\nu - \frac{T}{(u \cdot p)}\epsilon^{\mu\nu\alpha\beta}p_\alpha u_\beta \partial_\nu \frac{\mu}{T} + \frac{1}{(u \cdot p)}\epsilon^{\mu\nu\alpha\beta}p_\alpha u_\beta p^\sigma \partial_{<\sigma} u_{>}. \end{aligned} \quad (14)$$

In addition, given the equilibrium distribution functions in Eq. (5), we can rewrite the last term in \mathcal{J}_λ^μ as

$$2\pi\text{sign}(u \cdot p)\lambda\frac{\hbar}{4}\epsilon^{\mu\nu\alpha\beta}F_{\alpha\beta}\partial_\nu^p\delta(p^2)f_\lambda^{(0)} \approx -2\pi\text{sign}(u \cdot p)\lambda\frac{\hbar\delta(p^2)}{4}\epsilon^{\mu\nu\alpha\beta}F_{\alpha\beta}u_\nu\partial_{p \cdot u}f_\lambda^{(0)}, \quad (15)$$

up to $\mathcal{O}(\hbar)$. Note that in the above equation we have dropped the total derivative term, which is irrelevant to our current study.

For the convenience, we decompose the \mathcal{J}_5^μ as,

$$\mathcal{J}_5^\mu = \mathcal{J}_{\text{thermal}}^\mu + \mathcal{J}_{\text{shear}}^\mu + \mathcal{J}_{\text{accT}}^\mu + \mathcal{J}_{\text{chemical}}^\mu + \mathcal{J}_{\text{EB}}^\mu, \quad (16)$$

where

$$\begin{aligned} \mathcal{J}_{\text{thermal}}^\mu &= a\frac{1}{2}\epsilon^{\mu\nu\alpha\beta}p_\nu\partial_\alpha \frac{u_\beta}{T}, \\ \mathcal{J}_{\text{shear}}^\mu &= -a\frac{1}{(u \cdot p)T}\epsilon^{\mu\nu\alpha\beta}p_\alpha u_\beta p^\sigma \partial_{<\sigma} u_{>} \\ \mathcal{J}_{\text{accT}}^\mu &= -a\frac{1}{2T}\epsilon^{\mu\nu\alpha\beta}p_\nu u_\alpha (Du_\beta - \frac{1}{T}\partial_\beta T). \\ \mathcal{J}_{\text{chemical}}^\mu &= a\frac{1}{(u \cdot p)}\epsilon^{\mu\nu\alpha\beta}p_\alpha u_\beta \partial_\nu \frac{\mu}{T}, \\ \mathcal{J}_{\text{EB}}^\mu &= a\frac{1}{(u \cdot p)T}\epsilon^{\mu\nu\alpha\beta}p_\alpha u_\beta E_\nu + a\frac{B^\mu}{T}, \end{aligned} \quad (17)$$

with

$$a = 4\pi\hbar \text{sign}(u \cdot p) \delta(p^2) f_V^{(0)} (1 - f_V^{(0)}). \quad (18)$$

Note that

$$f_V^{(0)} = \frac{1}{2}(f_+^{(0)} + f_-^{(0)}), \quad (19)$$

and we have set the same chemical potential for both left and right fermions $\mu = \mu_+ = \mu_-$ for simplicity. The subscripts, *thermal*, *shear*, *accT*, *chemical* and *EB*, stand for the terms related to thermal vorticity, shear viscous tensor, the fluid acceleration minus gradient of temperature $Du_\mu - (\Delta_{\mu\nu}\partial^\nu T)/T$, the gradient of μ/T , and electromagnetic fields, respectively. Except for $\mathcal{J}_{\text{thermal}}^\mu$ and part of $\mathcal{J}_{\text{EB}}^\mu$ led by magnetic fields, all other terms in \mathcal{J}_5^μ come from the corrections beyond global equilibrium.

Let us take a close look at the $\mathcal{J}_{\text{accT}}^\mu$, which is usually neglected due to the following reason. One may utilize hydrodynamic equations of motion up to the order of \hbar or ∂^2 ,

$$\begin{aligned} DT &= -\frac{\epsilon + P}{p} \Delta^{\mu\nu} \partial_\nu u_\mu + \mathcal{O}(\hbar, \partial^2), \\ Du_\mu &= \frac{\Delta_{\mu\nu} \partial^\nu P}{\epsilon + P} + \mathcal{O}(\hbar, \partial^2), \\ D\bar{\mu}_{\text{R/L}} &= \mathcal{O}(\hbar, \partial^2), \end{aligned} \quad (20)$$

to replace the temporal derivatives D upon thermodynamic parameters, where ϵ and P correspond to the energy density and pressure, respectively. Here the \hbar corrections in Eq. (20) are irrelevant since they only contribute to higher-order terms at $\mathcal{O}(\hbar^2)$ in Wigner functions except for the off-equilibrium fluctuations led by collisions.

In the ideal limit, one of the hydrodynamic equations of motion becomes $Du_\mu = (\Delta_{\mu\nu}\partial^\nu T)/T$. Therefore, the $\mathcal{J}_{\text{accT}}^\mu$ vanishes in the ideal hydrodynamics. In the realistic hydrodynamic simulations, the dissipative corrections could further modify the evolution of Du_μ . In the viscous hydrodynamics, we have,

$$Du_\alpha = \frac{1}{\epsilon + P} \Delta_{\mu\alpha} \partial^\mu P - \frac{1}{\epsilon + P} \Delta_{\mu\alpha} \partial_\nu \pi^{\mu\nu} + \mathcal{O}(\hbar, \partial^3) \approx \frac{\Delta_{\mu\alpha}}{T} (\partial^\mu T - s^{-1} \partial_\nu \pi^{\mu\nu}), \quad (21)$$

where $\pi^{\mu\nu} = 2\Delta^{\mu\alpha} \Delta^{\nu\beta} \eta (\partial_{(\alpha} u_{\beta)} - g_{\alpha\beta} \partial_\rho u^\rho / 3) + \mathcal{O}(\partial^2)$ corresponds to the shear-stress tensor with η being the shear viscosity and s denotes the entropy density. Here we take $\epsilon + P = Ts$ and omit the correction from bulk viscosity for simplicity. We can further rewrite $\mathcal{J}_{\text{accT}}^\mu$ as

$$\mathcal{J}_{\text{accT}}^\mu = a \frac{1}{2T^2 s} \epsilon^{\mu\nu\alpha\beta} p_\nu u_\alpha \partial^\rho \pi_{\beta\rho} \approx a \frac{\eta}{T^2 s^2} \epsilon^{\mu\nu\alpha\beta} p_\nu u_\alpha \partial^\rho (s \hat{\pi}_{\beta\rho}), \quad (22)$$

where $\hat{\pi}^{\mu\nu} = \pi^{\mu\nu}/(2\eta)$ and we have assumed η/s is a constant to make the final approximation above. Consequently, we would like to emphasize here that the contributions from $\mathcal{J}_{\text{accT}}^\mu$ to the local spin polarization should depend on the EoS and parameter η/s . Note that in the early work [91], the authors have discussed the contribution from fluid acceleration Du_β implicitly involved in $\mathcal{J}_{\text{thermal}}^\mu$ to local polarization. Additionally, the magnetic-field contribution in $\mathcal{J}_{\text{EB}}^\mu$ has been also discussed in Ref. [10].

Although we discuss the polarization of massless fermions above, we may extend our analysis to massive fermions. In the case of massive fermions, we may generalize the on-shell condition $\delta(p^2)$ in Eq. (18) to $\delta(p^2 - m_i^2)$ with m_i being the mass of fermions. Then, we obtain the \mathcal{S}^μ in Eq. (2) from different sources,

$$\begin{aligned}
\mathcal{S}_{\text{thermal}}^\mu(\mathbf{p}) &= \frac{\hbar}{8m_\Lambda N} \int d\Sigma^\sigma p_\sigma f_V^{(0)} (1 - f_V^{(0)}) \epsilon^{\mu\nu\alpha\beta} p_\nu \partial_\alpha \frac{u_\beta}{T}, \\
\mathcal{S}_{\text{shear}}^\mu(\mathbf{p}) &= -\frac{\hbar}{4m_\Lambda N} \int d\Sigma \cdot p f_V^{(0)} (1 - f_V^{(0)}) \frac{\epsilon^{\mu\nu\alpha\beta} p_\alpha u_\beta}{(u \cdot p) T} \frac{1}{2} \{p^\sigma (\partial_\sigma u_\nu + \partial_\nu u_\sigma) - Du_\nu\} \\
\mathcal{S}_{\text{accT}}^\mu(\mathbf{p}) &= -\frac{\hbar}{8m_\Lambda N} \int d\Sigma \cdot p f_V^{(0)} (1 - f_V^{(0)}) \frac{1}{T} \epsilon^{\mu\nu\alpha\beta} p_\nu u_\alpha (Du_\beta - \frac{1}{T} \partial_\beta T), \\
\mathcal{S}_{\text{chemical}}^\mu(\mathbf{p}) &= \frac{\hbar}{4m_\Lambda N} \int d\Sigma \cdot p f_V^{(0)} (1 - f_V^{(0)}) \frac{1}{(u \cdot p)} \epsilon^{\mu\nu\alpha\beta} p_\alpha u_\beta \partial_\nu \frac{\mu}{T}, \\
\mathcal{S}_{\text{EB}}^\mu(\mathbf{p}) &= \frac{\hbar}{4m_\Lambda N} \int d\Sigma \cdot p f_V^{(0)} (1 - f_V^{(0)}) \left(\frac{1}{(u \cdot p) T} \epsilon^{\mu\nu\alpha\beta} p_\alpha u_\beta E_\nu + \frac{B^\mu}{T} \right), \tag{23}
\end{aligned}$$

where $N = \int d\Sigma^\mu p_\mu f_V^{(0)}$ and now $p^0 = \sqrt{|\mathbf{p}|^2 + m_i^2}$. In this work, we will only evaluate the spin polarization of Λ and neglect $\bar{\Lambda}$.

III. RESULTS AND DISCUSSION

A. Setup for Simulations

In this section, we implement the (3+1) dimensional viscous hydrodynamic CLVisc [92, 93] with AMPT initial conditions [16, 33, 94] to generate the freezeout hyper-surface and the profile of fluid velocity and temperature at that hyper-surface. Unless noted otherwise, we choose the EoS “*s95p-pce*” [95] instead of the EoS [96] used in Refs. [29, 88].

We introduce the polarization along the beam direction as $\mathcal{P}^z(p)$ and along the out-plane direction as $\mathcal{P}^y(p)$, which are obtained by integrating over the medium rapidity range

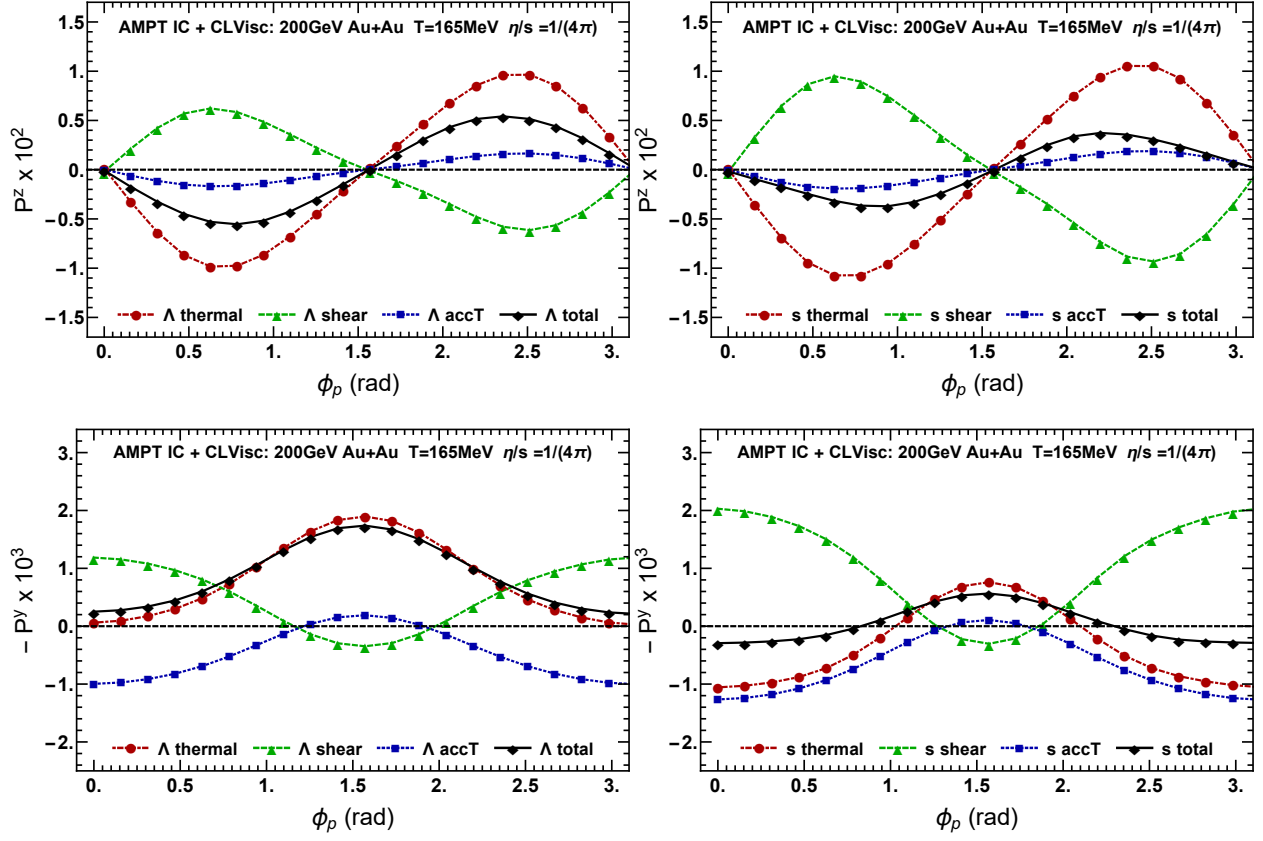


Figure 1: The polarization \mathcal{P}^z and \mathcal{P}^y as a function of ϕ_p for Λ and s equilibrium scenarios shown in the left and right panels. We have chosen $\eta/s = 1/(4\pi)$ and the freezeout temperature is 165 MeV. Red, green, and blue curves stand for the contributions from the thermal vorticity, shear induced polarization, and the acceleration terms, respectively. The black curve denotes the total polarization.

$[-1, +1]$,

$$\begin{aligned}\mathcal{P}^z(p) &= \int_{-1}^{+1} dY \mathcal{S}^z(p), \\ \mathcal{P}^y(p) &= \int_{-1}^{+1} dY \mathcal{S}^y(p),\end{aligned}\tag{24}$$

where \mathcal{S}^μ is given by Eqs. (23). We again use the subscripts, *thermal*, *shear*, *accT*, *chemical*, and *EB* for $\mathcal{P}^\mu(p)$ with $\mu = y, z$ to specify the contributions to the polarization from thermal vorticity, shear viscous tensor, $Du_\beta - \frac{1}{T}\partial_\beta T$, the gradient of μ/T , and electromagnetic fields, respectively.

Since the electromagnetic fields decay rapidly [97–99], we can neglect the contributions

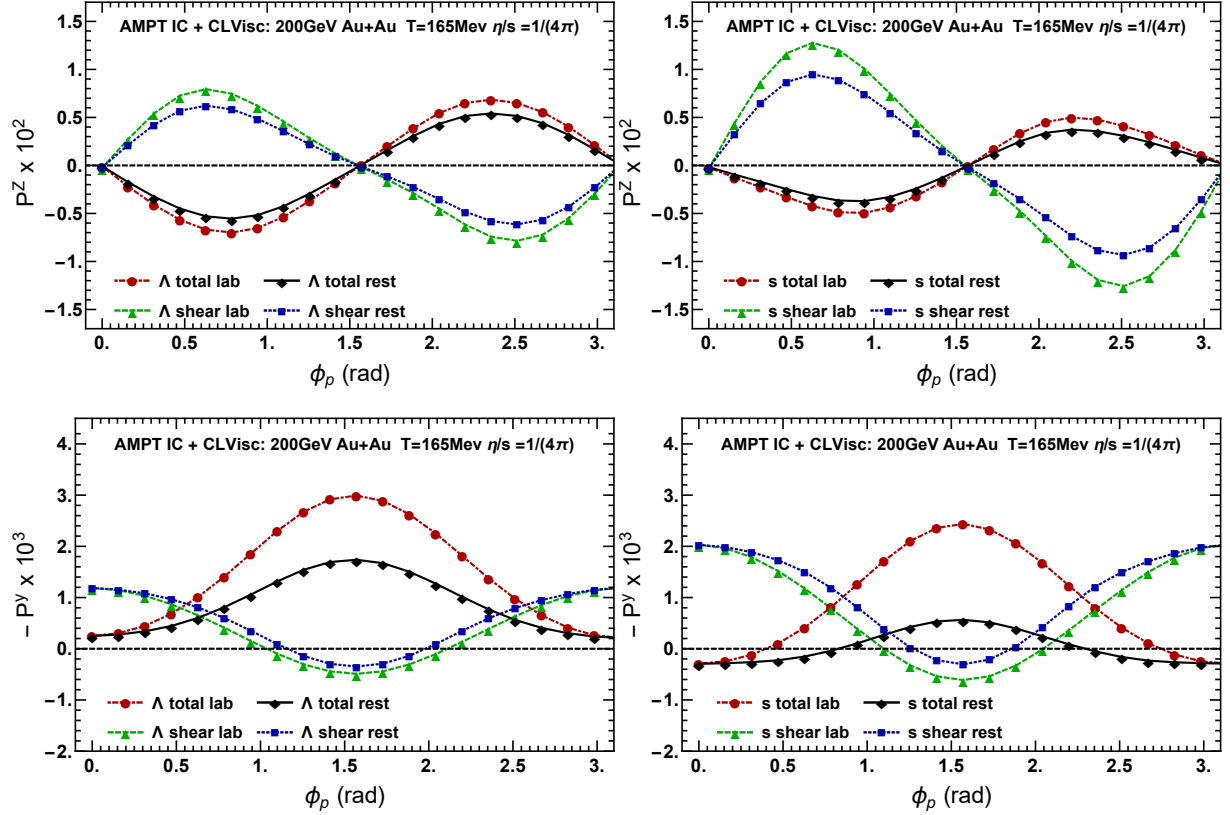


Figure 2: The polarization \mathcal{P}^z and \mathcal{P}^y as a function of ϕ_p for Λ hyperons and s quarks in the lab frame and their own rest frames. We have chosen $\eta/s = 1/(4\pi)$ and the freezeout temperature is 165 MeV. The red and black curves stand for the total polarization in the lab and the Λ (or s quark) rest frame, respectively. The green and blue curves denote the shear induced polarization in the lab and the Λ (or the s quark) rest frame, respectively.

from electromagnetic fields $\mathcal{S}_{\text{EB}}^\mu$ to the polarization vector $\mathcal{P}_{\text{EB}}^\mu$. Due to the limitation of the EoS in “*s95p-pce*”, we cannot get the sufficient information of chemical potential and its gradient. Therefore, in the current study, we will only consider the polarization induced by the thermal vorticity $\mathcal{S}_{\text{thermal}}^i$, shear viscous tensor $\mathcal{S}_{\text{shear}}^i$, and $\mathcal{S}_{\text{accT}}^i$ and evaluate

$$\mathcal{P}_{\text{total}}^\mu = \mathcal{P}_{\text{thermal}}^\mu + \mathcal{P}_{\text{shear}}^\mu + \mathcal{P}_{\text{accT}}^\mu. \quad (25)$$

The possible contribution from $\mathcal{S}_{\text{chemical}}^\mu$ will also be briefly discussed later.

We consider two scenarios in this work. In the first scenario, since the Λ hyperons are produced at the chemical freezeout, we assume that one can still utilize the macroscopic variables from hydrodynamics to describe the thermodynamical states of Λ hyperons, e.g.

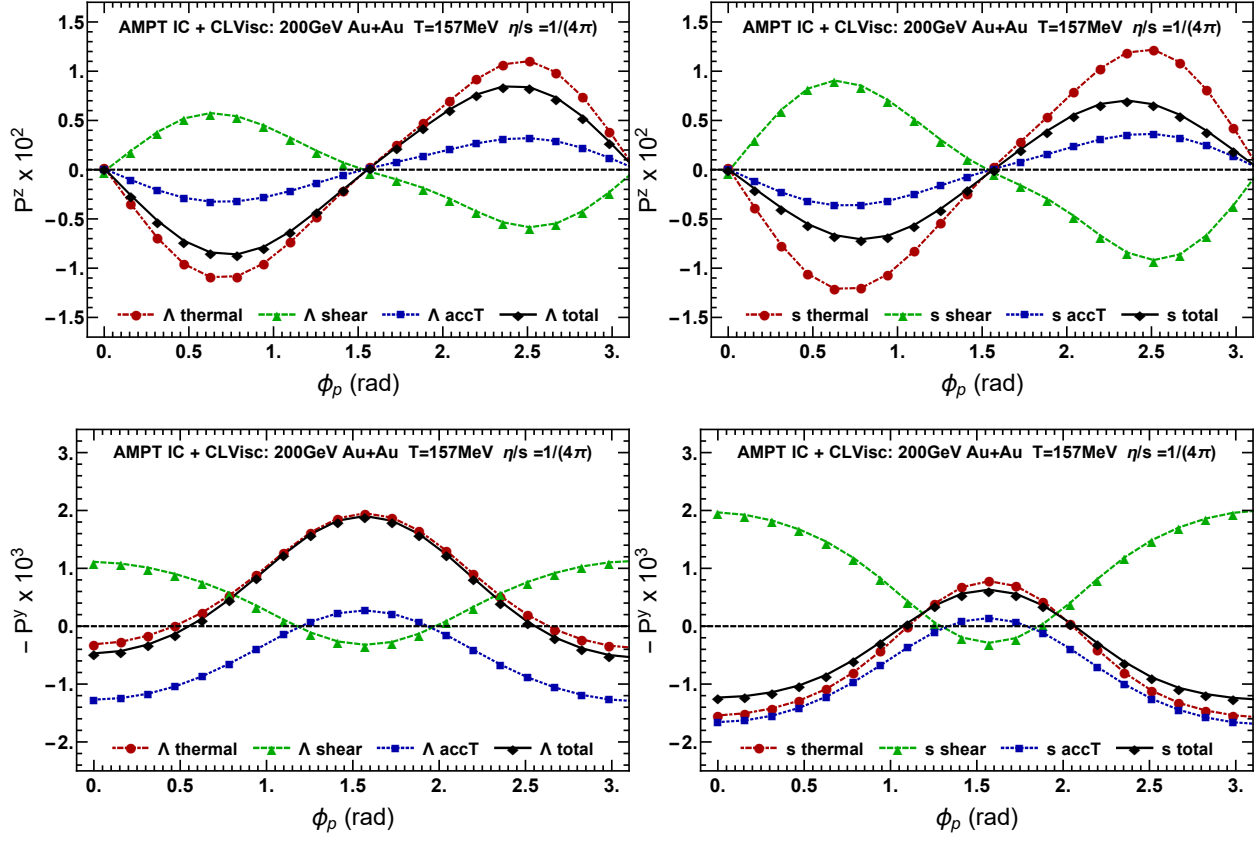


Figure 3: The same setup and color assignments as Fig. 1 except for changing the freezeout temperature to 157 MeV.

the temperature and its gradient, i.e. we assume that Λ hyperons are almost at local equilibrium. We name it as *Λ equilibrium scenario* for short.

In the second scenario, as proposed in Ref. [88], since the spin of s quark dominates over the total spin of Λ hyperon in the parton model, one can compute the polarization of s quarks and assume the spin polarization of the s quark is smoothly passed to the polarization of Λ . We name it as the *s equilibrium scenario*. Since the s quarks are much lighter than Λ hyperons, polarization induced by shear viscous tensor will be greatly enhanced in the s equilibrium scenario as opposed to the Λ equilibrium scenario, where $\mathcal{S}_{\text{shear}}^\mu$ is suppressed by $(u \cdot p) \sim m_\Lambda$ in the denominator shown in Eq. (23).

Note the polarization vectors in Eq. (24) are shown in the laboratory frame. In order to compare the results with the experimental data, we eventually transform them to the rest frame of the Λ hyperon for the Λ equilibrium scenario or of the s quark in the Λ hyperon for the s equilibrium scenario. In principle, we also need to consider the evolution of Λ hyperons

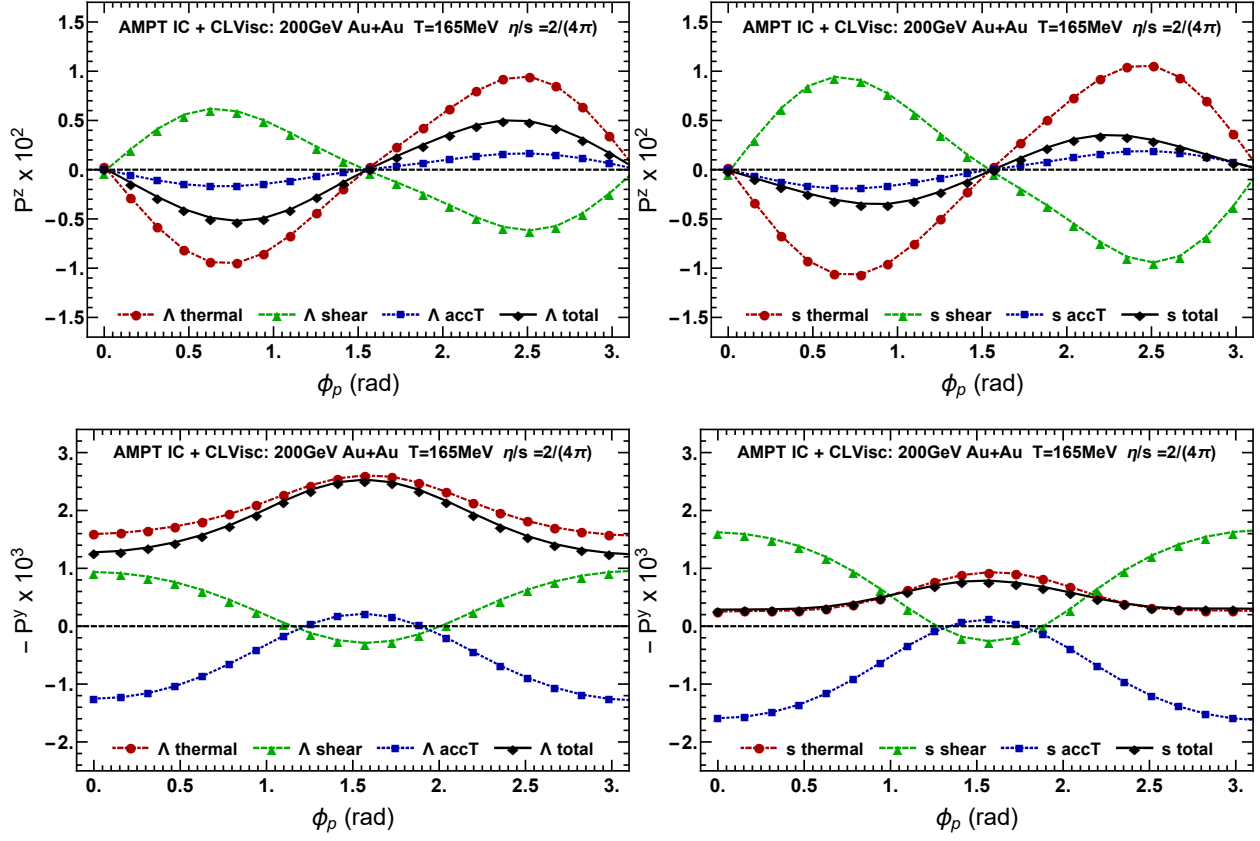


Figure 4: The same setup and color assignments as Fig. 1 except for changing the shear viscosity to entropy density ratio to $\eta/s = 2/(4\pi)$.

before kinetic freezeout, whereas we neglect the evolution of Λ hyperons after the chemical freezeout for simplicity.

We would like to emphasize that we always choose the factor m in the denominator of the right-hand side of Eq. (2) as m_Λ in both Λ and s equilibrium scenarios. The mass factor in Ref. [88] is instead chosen as m_s in the s equilibrium scenario, which will make an enhancement to the overall magnitude of polarization in the s equilibrium scenario. For numerical simulations, we choose $m_\Lambda = 1.116 \text{ GeV}$ for the mass of Λ hyperons and $m_s = 0.3 \text{ GeV}$ for the mass of constituent s quarks.

B. Numerical Results and Discussions

Here we briefly summarize the results presented in each figure. In Fig. 1, we show the local spin polarization coming from different sources in the lab frame. In Fig. 2, we compare

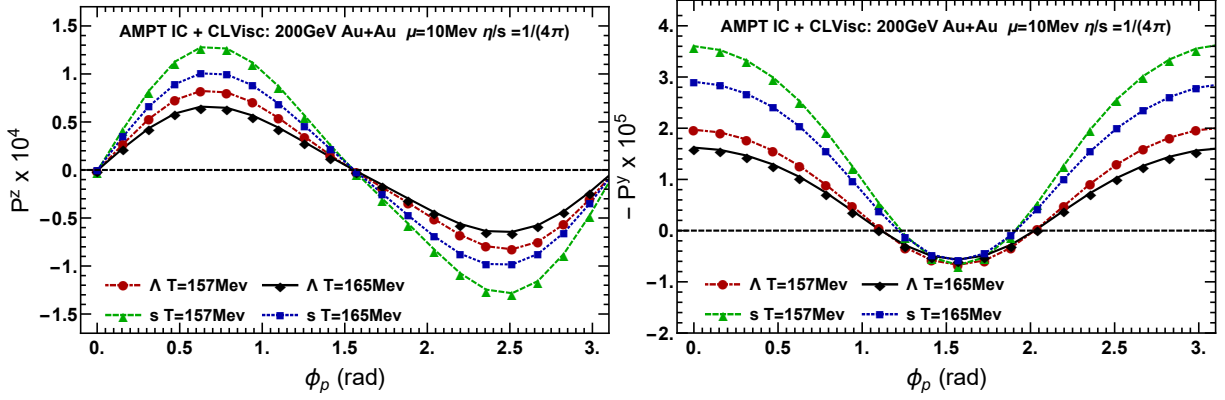


Figure 5: The polarization $10^4 \times \mathcal{P}_{\text{chemical}}^z$ and $10^5 \times \mathcal{P}_{\text{chemical}}^y$ as a function of ϕ_p for Λ and s equilibrium scenarios. We have chosen $\eta/s = 1/(4\pi)$ and the freezeout temperature as 165 MeV or 157 MeV. See color assignments for the results in the plots.

the results in the particles' rest frames to those in Fig. 1. In Fig. 3, we present the results with reduced freezeout temperature. In Fig. 4, the results with larger η/s but the same freezeout temperature as Fig. 1 are presented. Finally, we show the spin polarization led by a small and constant chemical potential from $\mathcal{P}_{\text{chemical}}^\mu$ for a heuristic discussion. The detailed results and discussions are presented below.

In Fig. 1, we plot the local spin polarization in both Λ and s equilibrium scenarios with $\eta/s = 1/(4\pi)$ and the freezeout temperature $T = 165$ MeV. We observe that the $\mathcal{S}_{\text{shear}}^\mu$ always leads to the “same” sign contribution, qualitatively consistent with experimental data, to the local spin polarization in both z and y directions and in the two scenarios. This observation is in accordance with Ref. [88]. Similar to thermal vorticity, $\mathcal{S}_{\text{accT}}^\mu$ induced by non-vanishing $Du_\mu - (\Delta_{\mu\nu}\partial^\nu T)/T$ leads to the “opposite” sign contribution to the local polarization. Along the beam direction, the magnitude of polarization $\mathcal{P}_{\text{accT}}^z$ is much smaller than the magnitudes of $\mathcal{P}_{\text{thermal}}^z$ and $\mathcal{P}_{\text{shear}}^z$ in the two scenarios. Along the out-plan direction, the $\mathcal{P}_{\text{accT}}^y$ is almost canceled with $\mathcal{P}_{\text{shear}}^y$ in Λ equilibrium scenario, while $|\mathcal{P}_{\text{accT}}^y| < |\mathcal{P}_{\text{shear}}^y|$ in the s equilibrium scenario. As a consequence of the competition between $\mathcal{P}_{\text{shear}}^\mu$ and $\mathcal{P}_{\text{thermal}}^\mu + \mathcal{P}_{\text{accT}}^\mu$, the $\mathcal{P}_{\text{total}}^{z,y}$ in both Λ and s equilibrium scenarios disagree with the experimental data.

In contrast, the hydrodynamic simulations in Ref. [88] find that the $\mathcal{P}_{\text{total}}^\mu$ in s equilibrium scenarios agree with the experimental data qualitatively. As mentioned previously, we have chosen a different EoS against the one in Ref. [88].

One possible reason leading to the different results may come from the following fact. In the EoS of *sp95-pce*, the speed of sound connecting QGP phase and PCE hadronic phase is not smooth and may lead to un-physical vorticity structure near to the freeze-out surface. We notice that the authors in Ref. [29] have studied the EoS dependence in the global polarization.

We have also checked the results by using another EoS *lattice-wb2014* [100] and the total polarization has a similar “sgin” as the experimental data qualitatively. But, $\mathcal{P}_{\text{total}}^{z,y}$ as a function of ϕ_p are almost flat $|\mathcal{P}_{\text{total}}^z|$ is quantitatively close to zero due to the highly suppression led by the factor m_Λ in the denominator of the right-hand side of Eq. (2). Therefore, our results show that the spin polarization with local-equilibrium corrections from hydrodynamic simulations are sensitive to the choice of EoS.

In Fig. 2, we compare the polarization in the laboratory frame and in particles’ rest frames. It is found the difference of the polarization in the two frames is mild for $\mathcal{P}_{\text{total}}^z$. Although the overall magnitudes and peaks of $\mathcal{P}_{\text{total}}^y$ are reduced in the particles’ rest frames, in general, the choices of frames do not change the polarization qualitatively.

Next, we consider the dependence of freezeout temperature. We set the freezeout temperature $T = 157$ MeV and keep $\eta/s = 1/(4\pi)$, and show the results in Fig. 3. The magnitudes of $\mathcal{P}_{\text{accT}}^\mu$ increase significantly when freezeout temperature decreases³. Since now $|\mathcal{J}_{\text{accT}}^\mu| \sim \mathcal{O}(T^{-2}p\partial^2)$ as a crude estimation for the magnitude of $\mathcal{J}_{\text{accT}}^\mu$ coming from the dissipative correction, it may be expected that $|\mathcal{P}_{\text{thermal}}^\mu|$ should increase with the reduced freezeout temperature.

On the other hand, we observe that the shear induced polarization $\mathcal{P}_{\text{shear}}^\mu$ is not sensitive to the freezeout temperature, while the magnitude of thermal vorticity induced polarization $\mathcal{P}_{\text{thermal}}^\mu$ is slightly enhanced. The difference between $\mathcal{P}_{\text{total}}^\mu$ in the two scenarios and experimental data increases due to the growth of the magnitude of $\mathcal{P}_{\text{accT}}^\mu$. It turns out that the $\mathcal{P}_{\text{total}}^\mu$ is also sensitive to the freezeout temperature.

Thirdly, we discuss the dependence of η/s . In Fig. 4, we set the $\eta/s = 2/(4\pi)$ and freezeout temperature $T = 165$ MeV. In comparison with the case of $\eta/s = 1/(4\pi)$ in Fig.

³ In fact, the magnitude of $\mathcal{P}_{\text{thermal}}^\mu$ also depends on the freezeout temperature since $\mathcal{J}_{\text{thermal}}^\mu$ implicitly incorporate the term related to Du^μ . But this term has been previously included in the hydrodynamic simulations for $\mathcal{P}_{\text{thermal}}^\mu$ in global equilibrium. It is worthwhile to note the full Wigner functions in local equilibrium, derived in Ref. [1], actually does not contain a term associated with Du^μ .

1, we find that all contributions to \mathcal{P}^z in the two scenarios have not changed much. On the contrary, the magnitudes of both $\mathcal{P}_{\text{thermal}}^y$ and $\mathcal{P}_{\text{accT}}^y$ in the two scenarios increase when η/s grows. The magnitudes of $\mathcal{P}_{\text{shear}}^y$ in the two scenarios become smaller than those in Fig. 1. Eventually, the $\mathcal{P}_{\text{total}}^y$ in the two scenarios are still different with the observation in experiments. It is found that the local polarization at least for $\mathcal{P}_{\text{total}}^y$ also depends on η/s .

At last, we compute the possible contribution from the gradient of chemical potential over temperature led by $\mathcal{S}_{\text{chemical}}^\mu$ in Eq. (23). For simplicity, we assume that the chemical potential is constant near the freezeout hypersurface and $\nabla\mu/T \simeq \mu\nabla(1/T)$. In Fig. 5, we choose the quark chemical potential $\mu = 10$ MeV. Similar to the shear viscous tensor, the $\mathcal{S}_{\text{chemical}}^\mu$ leads to the “same” sign contribution, qualitatively consistent with experimental data, to the local spin polarization in both z and y directions and in the two scenarios. However, $\mathcal{P}_{\text{chemical}}^\mu \propto \mu$ is highly suppressed by other contributions in $\mathcal{P}_{\text{total}}^\mu$. So far, they are almost negligible in the current study. However, $\mathcal{P}_{\text{chemical}}^\mu$ might be important in the low-energy collisions. We will leave it for the future studies.

As a concluding remark, we have shown that $\mathcal{P}_{\text{total}}^\mu$ is generally sensitive to EoS, freezeout temperature T , and the ratio η/s . We find that both $\mathcal{S}_{\text{shear}}^\mu$ and $\mathcal{S}_{\text{accT}}^\mu$ play important roles to local spin polarization. The behavior of $\mathcal{P}_{\text{total}}^\mu$ strongly depends on the predominant term in the competition between $\mathcal{P}_{\text{shear}}^\mu$ and $\mathcal{P}_{\text{thermal}}^\mu + \mathcal{P}_{\text{accT}}^\mu$. Although $\mathcal{S}_{\text{shear}}^\mu$ may lead to the “same” sign to the polarization, we still cannot get similar azimuthal angle dependence of local spin polarization as the experimental data with the EoS we have chosen.

IV. CONCLUSION

In this work, we first review the spin polarization (pesudo) vector $\mathcal{S}^\mu(\mathbf{p})$ derived from Wigner functions in Ref. [1]. We decompose $\mathcal{S}^\mu(\mathbf{p})$ into $\mathcal{S}_{\text{thermal}}^\mu, \mathcal{S}_{\text{shear}}^\mu, \mathcal{S}_{\text{accT}}^\mu, \mathcal{S}_{\text{chemical}}^\mu$ and $\mathcal{S}_{\text{EB}}^\mu$, which are led by thermal vorticity, shear viscous tensor, fluid acceleration minus the gradient of temperature, the gradient of chemical potential over temperature, and electromagnetic fields, respectively. We then implement of (3+1) dimensional viscous hydrodynamic CLVisc with AMPT initial conditions to obtain the numerical results for local spin polarization with zero electromagnetic fields and a vanishing chemical potential and focus on $\mathcal{P}_{\text{thermal}}^\mu, \mathcal{P}_{\text{shear}}^\mu$, and $\mathcal{P}_{\text{accT}}^\mu$ contributed by $\mathcal{S}_{\text{thermal}}^\mu, \mathcal{S}_{\text{shear}}^\mu$, and $\mathcal{S}_{\text{accT}}^\mu$. Inspired by Ref. [88], we also consider Λ and s equilibrium scenarios. As opposed to Ref. [88], we have chosen the

EoS “*s95p-pce*” as a different EoS and investigate the influence of η/s upon spin polarization.

Our numerical results show that both $\mathcal{P}_{\text{shear}}^\mu$ and $\mathcal{P}_{\text{accT}}^\mu$ affect $\mathcal{P}_{\text{total}}^\mu$ in addition to $\mathcal{P}_{\text{thermal}}^\mu$ that has been well studied in the literature. Although $\mathcal{P}_{\text{shear}}^\mu$ can lead to the “same” sign contribution, qualitatively consistent with experimental data, to the local spin polarization, $\mathcal{P}_{\text{accT}}^\mu$ also plays a crucial role and could change the behavior of $\mathcal{P}_{\text{total}}^\mu$ especially with lower freezeout temperature. It turns out that $\mathcal{P}_{\text{total}}^\mu$ is rather sensitive to EoS, η/s and freezeout temperature T . With the adopted EoS in our study, we do not observe the similar azimuthal angle dependence of local spin polarization as the experimental data.

We conclude that although the shear induced polarization alone may result in sizable effects on local spin polarization qualitatively consistent with experimental observations, it may not be always the dominant effect over other contributions in local equilibrium.

Although we have also checked the total local spin polarization by using another EoS and get the similar behavior as in Ref. [88], the total local spin polarization in s equilibrium scenario could still be highly suppressed if one chooses the m_Λ instead of m_s in the denominator of the right-hand side of Eq. (2).

Consequently, the so-called “sign” problem remains an open question. Moreover, from the theoretical perspective, the Wigner function in local equilibrium without the inclusion of off-equilibrium corrections pertinent to interaction is not a self-consistent solution for a kinetic equation. As indirectly supported by the influence from $\mathcal{P}_{\text{accT}}^\mu$, even in the near-equilibrium condition, the second-order gradient terms, such as the non-equilibrium corrections qualitatively studied in e.g. Refs. [1, 90] from CKT, may potentially give rise to sizable contributions in numerical simulations. To comprehensively investigate the spin polarization of fermions near local equilibrium and its direct connection to the “sign” problem, it will be still imperative to conduct the theoretical and numerical studies of spin hydrodynamics and the QKT with collisions.

Acknowledgments

We are grateful to thank Yi Yin, Longgang Pang, Shuai Y. F. Liu, Baochi Fu and Huichao Song for helpful discussions. S.P. is supported by National Nature Science Foundation of

China (NSFC) under Grants No. 12075235.

- [1] Y. Hidaka, S. Pu, and D.-L. Yang, Phys. Rev. **D97**, 016004 (2018), 1710.00278.
- [2] Z.-T. Liang and X.-N. Wang, Phys. Rev. Lett. **94**, 102301 (2005), nucl-th/0410079, [Erratum: Phys. Rev. Lett.96,039901(2006)].
- [3] Z.-T. Liang and X.-N. Wang, Phys. Lett. **B629**, 20 (2005), nucl-th/0411101.
- [4] F. Becattini and F. Piccinini, Annals Phys. **323**, 2452 (2008), 0710.5694.
- [5] F. Becattini, F. Piccinini, and J. Rizzo, Phys. Rev. C **77**, 024906 (2008), 0711.1253.
- [6] F. Becattini, V. Chandra, L. Del Zanna, and E. Grossi, Annals Phys. **338**, 32 (2013), 1303.3431.
- [7] Y. Jiang, Z.-W. Lin, and J. Liao, Phys. Rev. **C94**, 044910 (2016), 1602.06580, [Erratum: Phys. Rev.C95,no.4,049904(2017)].
- [8] W.-T. Deng and X.-G. Huang, Phys. Rev. **C93**, 064907 (2016), 1603.06117.
- [9] H. Li, L.-G. Pang, Q. Wang, and X.-L. Xia, Phys. Rev. C **96**, 054908 (2017).
- [10] R.-H. Fang, L.-G. Pang, Q. Wang, and X.-N. Wang, Phys. Rev. **C94**, 024904 (2016), 1604.04036.
- [11] D.-X. Wei, W.-T. Deng, and X.-G. Huang, Phys. Rev. C **99**, 014905 (2019).
- [12] L. Csernai, V. Magas, and D. Wang, Phys. Rev. C **87**, 034906 (2013), 1302.5310.
- [13] F. Becattini, L. Csernai, and D. Wang, Phys. Rev. C **88**, 034905 (2013), 1304.4427, [Erratum: Phys.Rev.C 93, 069901 (2016)].
- [14] F. Becattini *et al.*, Eur. Phys. J. C **75**, 406 (2015), 1501.04468, [Erratum: Eur.Phys.J.C 78, 354 (2018)].
- [15] L.-G. Pang, H. Petersen, Q. Wang, and X.-N. Wang, Phys. Rev. Lett. **117**, 192301 (2016), 1605.04024.
- [16] H.-Z. Wu, L.-G. Pang, X.-G. Huang, and Q. Wang, Nucl. Phys. A **1005**, 121831 (2021), 2002.03360.
- [17] B. Betz, M. Gyulassy, and G. Torrieri, Phys. Rev. C **76**, 044901 (2007), 0708.0035.
- [18] Y. B. Ivanov and A. A. Soldatov, Phys. Rev. C **95**, 054915 (2017).
- [19] Y. B. Ivanov and A. A. Soldatov, Phys. Rev. C **97**, 044915 (2018).
- [20] Y. B. Ivanov, V. D. Toneev, and A. A. Soldatov, Phys. Rev. C **100**, 014908 (2019).

- [21] I. Karpenko and F. Becattini, The European Physical Journal C **77**, 213 (2017).
- [22] Y. Xie, D. Wang, and L. P. Csernai, Phys. Rev. C **95**, 031901 (2017).
- [23] Y. Sun and C. M. Ko, Phys. Rev. **C96**, 024906 (2017), 1706.09467.
- [24] S. Shi, K. Li, and J. Liao, Physics Letters B **788**, 409 (2019).
- [25] STAR, L. Adamczyk *et al.*, Nature **548**, 62 (2017), 1701.06657.
- [26] STAR, J. Adam *et al.*, Phys. Rev. Lett. **123**, 132301 (2019), 1905.11917.
- [27] STAR, T. Niida, Nucl. Phys. A **982**, 511 (2019), 1808.10482.
- [28] F. Becattini and I. Karpenko, Phys. Rev. Lett. **120**, 012302 (2018).
- [29] B. Fu, K. Xu, X.-G. Huang, and H. Song, Phys. Rev. C **103**, 024903 (2021), 2011.03740.
- [30] X.-L. Xia, H. Li, Z.-B. Tang, and Q. Wang, Phys. Rev. C **98**, 024905 (2018), 1803.00867.
- [31] S. Y. F. Liu, Y. Sun, and C. M. Ko, (2019), 1910.06774.
- [32] Voloshin, Sergei A., EPJ Web Conf. **171**, 07002 (2018).
- [33] H.-Z. Wu, L.-G. Pang, X.-G. Huang, and Q. Wang, Phys. Rev. Research. **1**, 033058 (2019), 1906.09385.
- [34] X.-L. Xia, H. Li, X.-G. Huang, and H. Z. Huang, Phys. Rev. C **100**, 014913 (2019), 1905.03120.
- [35] F. Becattini, G. Cao, and E. Speranza, The European Physical Journal C **79**, 741 (2019).
- [36] R.-h. Fang, J.-y. Pang, Q. Wang, and X.-n. Wang, Phys. Rev. **D95**, 014032 (2017), 1611.04670.
- [37] M. A. Stephanov and Y. Yin, Phys. Rev. Lett. **109**, 162001 (2012), 1207.0747.
- [38] D. T. Son and N. Yamamoto, Phys. Rev. **D87**, 085016 (2013), 1210.8158.
- [39] J.-W. Chen, S. Pu, Q. Wang, and X.-N. Wang, Phys. Rev. Lett. **110**, 262301 (2013), 1210.8312.
- [40] C. Manuel and J. M. Torres-Rincon, Phys. Rev. **D89**, 096002 (2014), 1312.1158.
- [41] C. Manuel and J. M. Torres-Rincon, Phys. Rev. **D90**, 076007 (2014), 1404.6409.
- [42] J.-Y. Chen, D. T. Son, M. A. Stephanov, H.-U. Yee, and Y. Yin, Phys. Rev. Lett. **113**, 182302 (2014), 1404.5963.
- [43] J.-Y. Chen, D. T. Son, and M. A. Stephanov, Phys. Rev. Lett. **115**, 021601 (2015), 1502.06966.
- [44] Y. Hidaka, S. Pu, and D.-L. Yang, Phys. Rev. **D95**, 091901 (2017), 1612.04630.
- [45] N. Mueller and R. Venugopalan, Phys. Rev. **D97**, 051901 (2018), 1701.03331.

- [46] Y. Hidaka, S. Pu, and D.-L. Yang, Nucl. Phys. **A982**, 547 (2019), 1807.05018.
- [47] A. Huang, S. Shi, Y. Jiang, J. Liao, and P. Zhuang, Phys. Rev. **D98**, 036010 (2018), 1801.03640.
- [48] J.-H. Gao, Z.-T. Liang, Q. Wang, and X.-N. Wang, Phys. Rev. **D98**, 036019 (2018), 1802.06216.
- [49] Y.-C. Liu, L.-L. Gao, K. Mameda, and X.-G. Huang, Phys. Rev. **D99**, 085014 (2019), 1812.10127.
- [50] S. Lin and A. Shukla, JHEP **06**, 060 (2019), 1901.01528.
- [51] S. Lin and L. Yang, Phys. Rev. D **101**, 034006 (2020), 1909.11514.
- [52] N. Yamamoto and D.-L. Yang, Astrophys. J. **895**, 56 (2020), 2002.11348.
- [53] J.-H. Gao and Z.-T. Liang, Phys. Rev. **D100**, 056021 (2019), 1902.06510.
- [54] N. Weickgenannt, X.-L. Sheng, E. Speranza, Q. Wang, and D. H. Rischke, Phys. Rev. D **100**, 056018 (2019), 1902.06513.
- [55] K. Hattori, Y. Hidaka, and D.-L. Yang, Phys. Rev. **D100**, 096011 (2019), 1903.01653.
- [56] Z. Wang, X. Guo, S. Shi, and P. Zhuang, Phys. Rev. **D100**, 014015 (2019), 1903.03461.
- [57] D.-L. Yang, K. Hattori, and Y. Hidaka, JHEP **07**, 070 (2020), 2002.02612.
- [58] N. Weickgenannt, E. Speranza, X.-l. Sheng, Q. Wang, and D. H. Rischke, (2020), 2005.01506.
- [59] N. Weickgenannt, X.-L. Sheng, E. Speranza, Q. Wang, and D. H. Rischke, Wigner function and kinetic theory for massive spin-1/2 particles, in *28th International Conference on Ultra-relativistic Nucleus-Nucleus Collisions (Quark Matter 2019) Wuhan, China, November 4-9, 2019*, 2020, 2001.11862.
- [60] S. Li and H.-U. Yee, Phys. Rev. **D100**, 056022 (2019), 1905.10463.
- [61] Y.-C. Liu, K. Mameda, and X.-G. Huang, (2020), 2002.03753.
- [62] Z. Wang, X. Guo, and P. Zhuang, (2020), 2009.10930.
- [63] N. Weickgenannt, E. Speranza, X.-l. Sheng, Q. Wang, and D. H. Rischke, (2021), 2103.04896.
- [64] X.-L. Sheng, N. Weickgenannt, E. Speranza, D. H. Rischke, and Q. Wang, (2021), 2103.10636.
- [65] Z. Wang and P. Zhuang, (2021), 2105.00915.
- [66] J.-j. Zhang, R.-h. Fang, Q. Wang, and X.-N. Wang, Phys. Rev. C **100**, 064904 (2019), 1904.09152.
- [67] W. Florkowski, B. Friman, A. Jaiswal, and E. Speranza, Phys. Rev. C **97**, 041901 (2018).
- [68] W. Florkowski, E. Speranza, and F. Becattini, Acta Phys. Polon. B **49**, 1409 (2018),

- 1803.11098.
- [69] D.-L. Yang, Phys. Rev. D **98**, 076019 (2018), 1807.02395.
 - [70] F. Becattini, W. Florkowski, and E. Speranza, Physics Letters B **789**, 419 (2019).
 - [71] W. Florkowski, R. Ryblewski, and A. Kumar, Prog. Part. Nucl. Phys. **108**, 103709 (2019), 1811.04409.
 - [72] K. Hattori, M. Hongo, X.-G. Huang, M. Matsuo, and H. Taya, Phys. Lett. B **795**, 100 (2019), 1901.06615.
 - [73] S. Bhadury, W. Florkowski, A. Jaiswal, A. Kumar, and R. Ryblewski, (2020), 2002.03937.
 - [74] S. Shi, C. Gale, and S. Jeon, Phys. Rev. C **103**, 044906 (2021), 2008.08618.
 - [75] D. Montenegro, L. Tinti, and G. Torrieri, Phys. Rev. D **96**, 076016 (2017), 1703.03079.
 - [76] D. Montenegro, L. Tinti, and G. Torrieri, Phys. Rev. D **96**, 056012 (2017), 1701.08263, [Addendum: Phys.Rev.D 96, 079901 (2017)].
 - [77] S. Li, M. A. Stephanov, and H.-U. Yee, (2020), 2011.12318.
 - [78] K. Fukushima and S. Pu, (2020), 2001.00359.
 - [79] K. Fukushima and S. Pu, Phys. Lett. B **817**, 136346 (2021), 2010.01608.
 - [80] A. D. Gallegos, U. Gürsoy, and A. Yarom, (2021), 2101.04759.
 - [81] Q. Wang, Nucl. Phys. A **967**, 225 (2017), 1704.04022.
 - [82] F. Becattini and M. A. Lisa, Ann. Rev. Nucl. Part. Sci. **70**, 395 (2020), 2003.03640.
 - [83] F. Becattini, Polarization in relativistic fluids: a quantum field theoretical derivation, 2020, 2004.04050.
 - [84] J.-H. Gao, G.-L. Ma, S. Pu, and Q. Wang, Nucl. Sci. Tech. **31**, 90 (2020), 2005.10432.
 - [85] Y.-C. Liu and X.-G. Huang, Nucl. Sci. Tech. **31**, 56 (2020), 2003.12482.
 - [86] S. Y. F. Liu and Y. Yin, (2020), 2006.12421.
 - [87] S. Y. F. Liu and Y. Yin, (2021), 2103.09200.
 - [88] B. Fu, S. Y. F. Liu, L. Pang, H. Song, and Y. Yin, (2021), 2103.10403.
 - [89] F. Becattini, M. Buzzegoli, A. Palermo, G. Inghirami, and I. Karpenko, (2021), 2103.14621.
 - [90] Y. Hidaka and D.-L. Yang, Phys. Rev. D **98**, 016012 (2018), 1801.08253.
 - [91] I. Karpenko and F. Becattini, Nucl. Phys. A **982**, 519 (2019), 1811.00322.
 - [92] L. Pang, Q. Wang, and X.-N. Wang, Phys. Rev. C **86**, 024911 (2012), 1205.5019.
 - [93] L.-G. Pang, H. Petersen, and X.-N. Wang, Phys. Rev. C **97**, 064918 (2018), 1802.04449.
 - [94] Z.-W. Lin, C. M. Ko, B.-A. Li, B. Zhang, and S. Pal, Phys. Rev. C **72**, 064901 (2005),

nucl-th/0411110.

- [95] P. Huovinen and P. Petreczky, Nucl. Phys. A **837**, 26 (2010), 0912.2541.
- [96] G. S. Denicol *et al.*, Phys. Rev. C **98**, 034916 (2018), 1804.10557.
- [97] J. Bloczynski, X.-G. Huang, X. Zhang, and J. Liao, Phys. Lett. **B718**, 1529 (2013), 1209.6594.
- [98] W.-T. Deng and X.-G. Huang, Phys. Rev. **C85**, 044907 (2012), 1201.5108.
- [99] V. Roy and S. Pu, Phys. Rev. **C92**, 064902 (2015), 1508.03761.
- [100] S. Borsanyi *et al.*, Phys. Lett. B **730**, 99 (2014), 1309.5258.